ALFVEN WAVE SIGNATURE FROM CONSTANT-CURRENT TETHERS

Robert D. Estes
Harvard-Smithsonian Center for Astrophysics, 60 Garden St., Cambridge, MA 02138

Juan R. Sanmartín
ETSI Aeronáuticos, Universidad Politécnica de Madrid, 28040 Madrid, Spain

The Alfvén wave signature left far behind in the ionosphere by tethers operating as thrusters or generators is analyzed. A recent description of tether radiation is used to determine the far-field in the ionosphere. It is shown that the Alfvén wings have an Airy function crosswise structure (a feature common to other wavefronts and now identified in published numerical results on Alfvén waves), with the field amplitude weakly decaying as the inverse cubic root of distance along the fronts. This corrects and completes a previous far-field analysis, which holds behind the wings.

In the standard picture of a tethered satellite system that has a steady electrical current flowing through it by means of continual charge exchange with the ambient plasma, "circuit closure" is accomplished by charge-carrying electromagnetic waves excited in the ionosphere by the passage of the system. The dual constraints of steady-state operation (Döppler condition) and satisfaction of the plasma wave dispersion relation are quite stringent and, as demonstrated by Barnett and Olbert[1], greatly restrict the types and frequency ranges of waves available for circuit closure. We note in particular that whistler waves, which have been observed in plasma chamber experiments meant to model the operation of a tethered system[2], do not satisfy the criteria for propagating waves from a constant-current tether orbiting the Earth[3].

Among the propagating waves that can be excited by a constant-current tether are those lying on the Alfvén branch with frequencies below the ion cyclotron frequency. Alfvén wave packets associated with the motion of a large conductor moving through a magnetoplasma and which serve to carry current in the ionospheric transmission line, completing the electrical circuit that includes the moving conductor, were first described theoretically by Drell *et al.*[4] in 1965. Since then a number of authors[1,3,5-8] have considered the so-called "Alfvén wings" with particular application to tethers in space.

Ground-based measurements of electromagnetic signals associated with tether-induced ionospheric waves have been attempted during the PMG experiment and will be attempted during TSS-1R. The use of properly equipped satellites already in orbit to measure waves from TSS-1R in the ionosphere is a possibility being actively pursued at present. It is thus desirable to have a good theoretical representation of the plasma waves associated with the tether hundreds of kilometers from the system to guide the planning of data collection and analysis, which could in turn help validate the theory.

The present work is a step in that direction. We obtain far-field values of the Alfvén wing field components and the general shape of these wing structures. Rasmussen *et al.*[6] have also derived asymptotic approximations to part of the tether Alfvén waves, and we compare our results to theirs below.

We consider a tethered satellite system orbiting in a magnetized plasma and consisting of a conducting tether with terminating contactors, where we use the term generically to include metallic surfaces in electrical contact with the tether and exposed to the ambient plasma as well as plasma devices such as hollow cathodes which define the regions of charge exchange between the tethered system and the ionosphere.

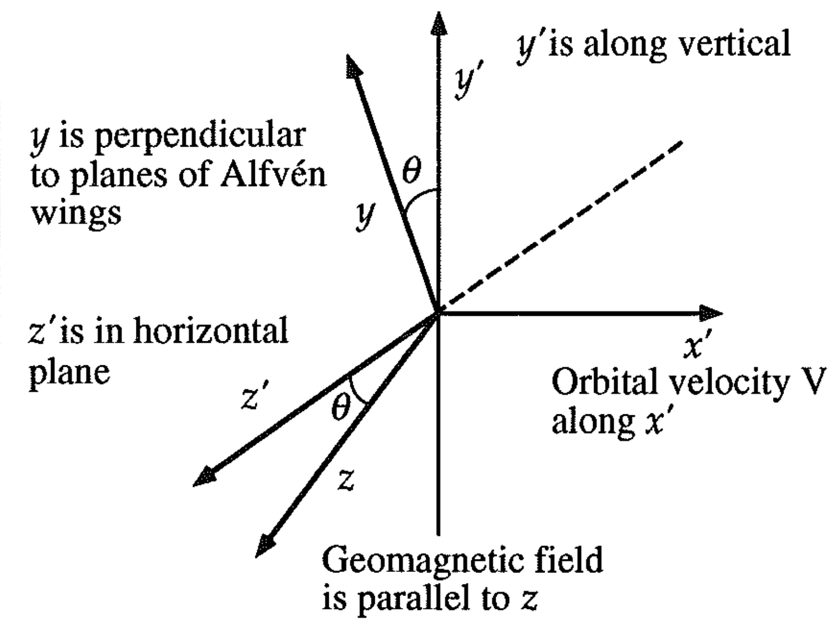

Figure 1—Co-ordinate systems used in the analysis

Our calculations use cold-plasma theory and assume an infinite, uniform ionosphere and a constant background magnetic field. Motion of the system is taken to be linear with a constant speed. The geomagnetic field is perpendicular to the system's velocity vector, but it is allowed to tilt at an arbitrary angle with respect to the horizontal. (See Figure1). The tether is vertical.

Results apply equally to a system operating in the thruster or generator mode. We are not studying transient effects that may occur when the tether is first "turned on", *e.g.*, when current flow is activated by closing a switch; rather we assume that a steady state has been reached in which a constant current is flowing in the tether with charge-exchange taking place between the system and the ionosphere through the terminating contactors. This implies that the plasma has adjusted to the presence of the tethered system so that, in the rest frame of the tether, currents and fields measured in the system or the plasma are constant in time at any point fixed relative to the origin of the tether co-ordinate system.

Thus in the tether rest frame an observer sees a steady "structure" of fields and currents extending indefinitely into the plasma. The situation is rather like an idealized version of the bow wave of a boat, which appears unvarying when viewed from the boat. From the standpoint of the plasma things seem far more dynamic. As the tether approaches, plasma upstream from the system begins to feel the effects of the tethered system's perturbation in the form of the fields and currents induced in the plasma closer to the system. At a given point in the plasma rest frame, the fields and currents will vary (markedly for a point near the track of one of the terminating contactors) as the system passes by.

As we are interested in the Alfvén wings, we restrict consideration to frequencies below the ion cyclotron frequency Ω_i and follow the method introduced in reference 3, which expresses the electrostatic potential for propagating waves in this frequency range as

$$\phi(\mathbf{r}) = \frac{I}{\pi}\iiint \frac{d^3k\; g(\mathbf{k})e^{i\mathbf{k}\cdot\mathbf{r}}}{\omega k_\perp^2\left(\varepsilon_1(\omega) - \left(\frac{ck_z}{\omega}\right)^2\right)}, \tag{1}$$

where $\mathbf{r} = (x - Vt, y, z)$ with V being the tether velocity. The time-dependence is contained in the exponential, and it should be understood that $\omega = k_x V$, this equality being the mathematical expression of the steady-state condition.

Electric field components perpendicular to the geomagnetic field are the corresponding derivatives of the potential. Magnetic field components follow directly from the electric field. This formulation, while equivalent to others previously used, emphasizes the electrostatic nature of the phenomenon of tether-induced waves. These charge-carrying waves are excited by the regions of net charge being continualy created in the plasma at the terminating contactors of the tether as the plasma flows by.

The physics of the plasma response is largely governed by the diagonal components perpendicular to the magnetic field of the cold-plasma dielectric tensor

$$\varepsilon_1(\omega) \approx \frac{c^2}{V_A^2} \frac{1}{1-(\omega/\Omega_i)^2}, \tag{2}$$

where V_A is the Alfvén speed and c the speed of light; while the tethered system's excitation of the plasma is contained in the factor

$$g(\mathbf{k}) \equiv \frac{-i}{2\pi I} \iiint d^3x \, \nabla \cdot \mathbf{j}_{source} e^{-i\mathbf{k}\cdot\mathbf{x}}, \tag{3}$$

where $\mathbf{j}_{source}$ is the current density in the tethered system and I is the tether current.

For computational convenience we consider the case where the contactor dimension along the direction of flight $L_x << V/\Omega_i \approx 36m$ (in the F-region of the ionosphere). This is an appropriate approximation for the TSS-1R satellite. In this case we have

$$g \approx \frac{1}{\pi}\sin\left(\frac{k_y' L}{2}\right) = \frac{1}{\pi}\sin\left(\frac{L}{2}\left(k_y \cos\theta - k_z \sin\theta\right)\right), \tag{4}$$

where L is the length of the tether.

For what follows it is convenient to define a number of quantitiies:

$$\bar{x}_i \equiv x_i \frac{\Omega_i}{V},$$

$$E_0 \equiv \frac{\Omega_i V_A}{Vc^2} I, \quad \bar{E}_i \equiv \frac{E_i}{E_0},$$

$$\bar{Y}_{+,-} \equiv \bar{y} \pm \tfrac{1}{2}\bar{L}\cos\theta, \text{ and } \bar{Z}_{+,-} \equiv \bar{z} \pm \tfrac{1}{2}\bar{L}\sin\theta.$$

The integrals over k_y and k_z in (1) can be carried out easily by applying residue theory to obtain the following expressions for the electric field components (for $Z > 0$):

$$\bar{E}_x = F(\bar{Y}_-, \bar{Z}_+) - F(\bar{Y}_+, \bar{Z}_-) \tag{5}$$

and

$$\overline{E}_y = G(\overline{Y}_-,\overline{Z}_+) - G(\overline{Y}_+,\overline{Z}_-), \tag{6}$$

where the first terms correspond to the contibutions of the top contactor, the second terms to those of the bottom contactor, and

$$F(\overline{Y},\overline{Z}) = \int_0^1 d\kappa\ \sqrt{1-\kappa^2}e^{-\kappa|\overline{Y}|}\sin\left(\kappa\left[\overline{x}+\overline{Z}\frac{V/V_A}{\sqrt{1-\kappa^2}}\right]\right) \tag{7}$$

and

$$G(\overline{Y},\overline{Z}) = \int_0^1 d\kappa\ \sqrt{1-\kappa^2}e^{-\kappa|\overline{Y}|}\operatorname{sgn}(\overline{Y})\cos\left(\kappa\left[\overline{x}+\overline{Z}\frac{V/V_A}{\sqrt{1-\kappa^2}}\right]\right) \tag{8}$$

For $\theta = 0$, these expressions reduce to the corresponding quantities derived in reference 5 (when the small contactor limit is taken). The Alfvén wings are wave packets composed of frequencies up to Ω_i. Near the tethered system they start out as rather compact structures with significant fields and currents largely confined to regions within a hundred meters or so of the contactors (for the small contactors we are considering). But as they travel away from the system the wings progressively lose their coherence because wave components of different frequencies have different phase velocites, a consequence of expression (2). The leading edges of the wings become progressively sharper, while "ripples" in the wake become more extensive and attain greater amplitudes[5].

The fields obtained above in equations (5)-(8) can be evaluated by numerical integration. This can be time-consuming without necessarily being illuminating, however. There is considerable virtue in having approximate expressions that are more easily understood and which elucidate the general behavior of the solutions, particularly if they are easier to calculate. We now obtain such useful asymptotic approximations in two different domains far from the tethered system.

Let us first consider the far field near the leading edge of the wings, which is of primary interest from the standpoint of experimental measurement. This is defined by the conditions that $|\overline{x}|$ is very large, while

$$(V/V_A)\overline{Z}/|\overline{x}| \cong 1\,. \tag{9}$$

Far from the tether components with $\omega << \Omega_i$ ($\kappa<<1$) dominate in this region. Thus we take

$$\kappa\left(\overline{x}+\overline{Z}\frac{V/V_A}{\sqrt{1-\kappa^2}}\right) \cong \kappa\left(\overline{x}+(V/V_A)\overline{Z}(1+\tfrac{1}{2}\kappa^2)\right) \cong \kappa\left(\overline{x}+(V/V_A)\overline{Z}\right)+\tfrac{1}{2}\kappa^3|\overline{x}| \tag{10}$$

in the arguments in (7) and (8). Neglecting κ^2 in the square root factor, we make the substitutions

$$s \equiv (\tfrac{3}{2}|\overline{x}|)^{\frac{1}{3}}\kappa \quad \text{and} \quad \zeta \equiv \frac{\overline{x}+(V/V_A)\overline{Z}}{(\tfrac{3}{2}|\overline{x}|)^{\frac{1}{3}}} \tag{11}$$

and extend the upper limit of the s integration to infinity, which we justify by the assumption of large $|\overline{x}|$

and the highly oscillatory integrand, to obtain

$$F \cong \left(\tfrac{3}{2}|\overline{x}|\right)^{-\frac{1}{3}} \int_0^\infty ds \ \exp\left(\frac{-s|\overline{Y}|}{\left(\frac{3}{2}|\overline{x}|\right)^{\frac{1}{3}}}\right) \sin\left(\zeta s + \tfrac{1}{3}s^3\right) \tag{12}$$

and

$$G \cong \left(\tfrac{3}{2}|\overline{x}|\right)^{-\frac{1}{3}} \int_0^\infty ds \ \exp\left(\frac{-s|\overline{Y}|}{\left(\frac{3}{2}|\overline{x}|\right)^{\frac{1}{3}}}\right) \operatorname{sgn}(\overline{Y}) \cos\left(\zeta s + \tfrac{1}{3}s^3\right) \ . \tag{13}$$

In the plane of the top or bottom Alfvén wing (*i.e.*, for $\overline{Y} \to 0$) we have simply

$$G \cong \left(\tfrac{3}{2}|\overline{x}|\right)^{-\frac{1}{3}} \pi \operatorname{sgn}(\overline{Y}) \tfrac{1}{\pi} \int_0^\infty ds \ \cos\left(\zeta s + \tfrac{1}{3}s^3\right) = \left(\tfrac{3}{2}|\overline{x}|\right)^{-\frac{1}{3}} \pi \operatorname{sgn}(\overline{Y}) \operatorname{Ai}(\zeta) \ , \tag{14}$$

where Ai is one of the Airy integrals[9]. A similar expression holds true for F and the Airy integral Gi[9].

$$F \cong \left(\tfrac{3}{2}|\overline{x}|\right)^{-\frac{1}{3}} \pi \tfrac{1}{\pi} \int_0^\infty ds \ \sin\left(\zeta s + \tfrac{1}{3}s^3\right) = \left(\tfrac{3}{2}|\overline{x}|\right)^{-\frac{1}{3}} \pi \operatorname{Gi}(\zeta) \tag{15}$$

This asymptotic behavior is a feature common to other wavefronts (See, *e.g.*, reference 10). A transition toward this behavior can be seen already in the figures displaying fields and currents in refer-

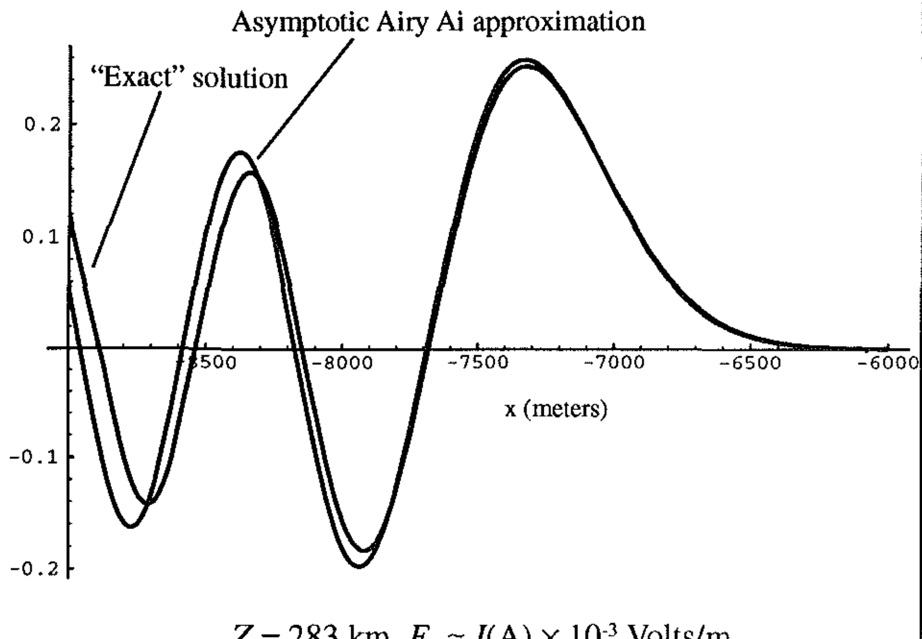

$Z_+ = 283$ km, $E_0 \approx I(\mathrm{A}) \times 10^{-3}$ Volts/m

Figure 2—Comparison of asymptotic Alfvén wing solution and numerically integrated exact solution of E_y/E_0

ence 5 for points too near the tether to be in the asymptotic region.

Figure 2 displays a comparison between the values of $\overline{E}_y$ obtained by numerical integration of expression (8) and the approximation of expression (14) for points in the top Alfvén wing some 283 km away from the top contactor. Agreement is seen to be quite good for a distance of about 2 km along the x axis. The "exact" solution decays with x more rapidly than the approximation. Even beyond the region of good agreement the approximation continues to provide a useful qualitative picture of the variation in the field component in the plane of the wing. Thus the approximation does all we ask of it in terms of accuracy. It also succeeds in the area of speed and convenience. The Airy function curve in Figure 2 required seconds to generate, while the numerically integrated curve required minutes. The approximation to $\overline{E}_x$ of (15) is shown in Figure 3 for the same distance from the contactor in the top wing.

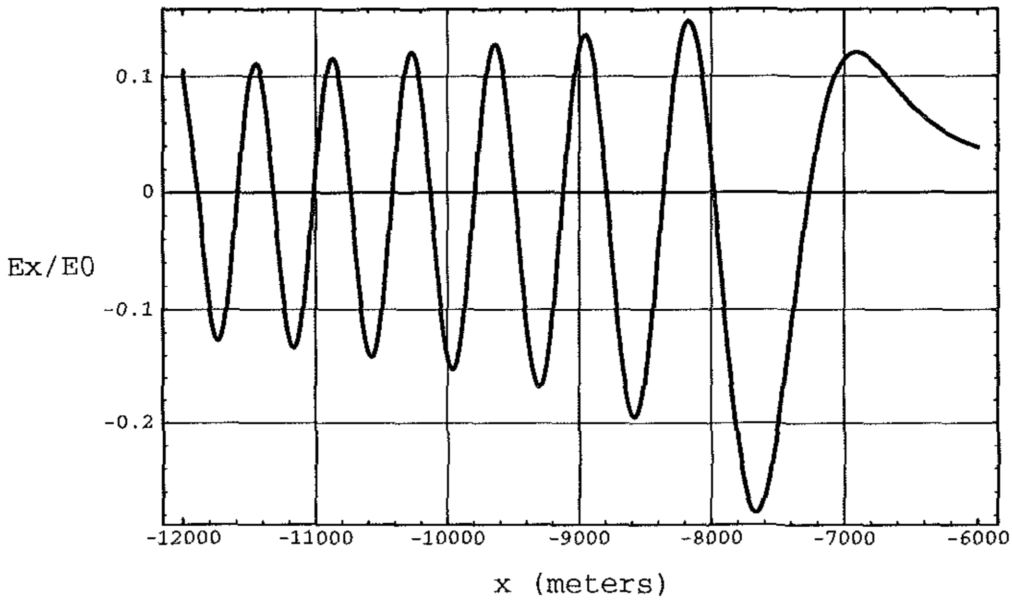

Figure 3—Asymptotic approximation to E_x/E_0 in the plane of the top Alfvén wing at a distance of 283 km from the top contactor.

The asymptotic approximation reveals other general features of the far-field wing structure. As we can see from (12) and (13), amplitudes decay across the wing according to the inverse cube root of the distance behind the contactor (*i.e.*, $|\bar{x}|^{-\frac{1}{3}}$), although, as we have seen in the example of Figure 2, this somewhat underestimates the rate of decay as we get away from the leading edge of the wing.

Another observation we can make from the asymptotic solution is that the wings, while maintaining their general shape with increasing distance from the contactor, undergo a general broadening, *i.e.*, peaks broaden, etc. This broadening is due to the progressive loss of higher frequency, shorter wavelength, components, as noted in reference 6. This broadening occurs proportionally to the cube-root of $|\bar{x}|$, which follows from the scaling of the Airy function argument defined in (11).

We now turn our attention to the far field well behind the wings. Although, strictly speaking, there is no well-defined back edge to the wings, Rasmussen *et al.*[6] pointed out that far behind the leading edge of a wing, along a given ray (defined by constant Z/x) and far enough away from the contactor, only wave components close to a single well-defined frequency are found to radiate. We now obtain an asymptotic approximation appropriate to this region by applying the method of stationary phase to the integrals in expresssions (7) and (8).

This method depends upon the integrand's being highly oscillatory for large values of $|\bar{x}|$, which implies certain conditions on x/Z. Only a narrow range of κ values around the stationary point of the argument of the sinusoidal function then contributes significantly to the integral. We define $f(\kappa)$ by

$$|\overline{x}|f(\kappa) \equiv \kappa\left(\overline{x} + \overline{Z}\frac{V/V_A}{\sqrt{1-\kappa^2}}\right) \tag{16}$$

and look for stationary points of

$$f(\kappa) = -\kappa + \frac{\kappa V/V_A}{\sqrt{1-\kappa^2}}\overline{Z}/|\overline{x}| \tag{17}$$

defined by $f'(\kappa_*) = 0$, which occur for

$$1-\kappa_*^2 = \left[(V/V_A)\overline{Z}/|\overline{x}|\right]^{2/3}, \tag{18}$$

so that $f(\kappa_*) = -\kappa_*^3$, which shows the method is applicable only if

$$\kappa_*^3|\overline{x}| >> 1 \tag{19}$$

or

$$\left(1-\left[(V/V_A)\overline{Z}/|\overline{x}|\right]^{2/3}\right)^{3/2}|\overline{x}| >> 1. \tag{20}$$

We have further that

$$f_*'' \equiv f''(\kappa_*) = 3\kappa_*/\left(1-\kappa_*^2\right). \tag{21}$$

Then, in the neighborhood of the stationary point

$$f(\kappa) \cong -\kappa_*^3 + \tfrac{1}{2}f_*''\Delta\kappa^2, \text{ where } \Delta\kappa \equiv \kappa - \kappa_* . \tag{22}$$

We change the variable of integration to

$$s \equiv \sqrt{\tfrac{1}{2}|\overline{x}|f_*''}\Delta\kappa , \tag{23}$$

extend the limits of integration, and extract the non-oscillatory factor from the the integrand (evaluating it at the stationary point) to obtain

$$F \cong \sqrt{\frac{2}{|\overline{x}|}}\sqrt{\frac{1-\kappa_*^2}{f_*''}}e^{-\kappa_*|\overline{y}|}\int_{-\infty}^{\infty} ds\ \sin\left(\overline{x}\kappa_*^3 + s^2\right). \tag{24}$$

The integral is well known, and with substitutions we finally obtain

$$F \cong \sqrt{\tfrac{2\pi}{3}}\frac{\left[(V/V_A)\bar{Z}/|\bar{x}|\right]^{2/3}}{\sqrt{|\bar{x}|\kappa_*}}e^{-\kappa_*|\bar{Y}|}\sin\left(\bar{x}\kappa_*^3+\tfrac{\pi}{4}\right) \tag{25}$$

for the far field behind the wings. Similarly,

$$G \cong \sqrt{\tfrac{2\pi}{3}}\frac{\left[(V/V_A)\bar{Z}/|\bar{x}|\right]^{2/3}}{\sqrt{|\bar{x}|\kappa_*}}e^{-\kappa_*|\bar{Y}|}\operatorname{sgn}(\bar{Y})\cos\left(\bar{x}\kappa_*^3+\tfrac{\pi}{4}\right). \tag{26}$$

Rasmussen *et al.*[6] applied the stationary-phase method to obtain results similar to (25)-(26) for a special tether current distribution, ignoring phase factors. They found, in particular, the amplitude along a ray of constant $|Z/x|$ to decay as the inverse square-root of the distance $r=\sqrt{x^2+Z^2}$ from the contactor in the x-z plane, which agrees with our results far back in the wake. They also found the far-field narrow-band radiation around a frequency $\omega_* \equiv \kappa_*\Omega_i$ to be at an angle, defined by constant $|Z/x|$ such that our equation (18) was satisfied.

However, we do not agree with some of the interpretations of Rasmussen, *et al.*[6] They identify the region in which their stationary-phase results are valid as the "far field". Actually, a far-field analysis is valid for all $|\bar{x}|>>1$. As we have seen, the stationary-phase results apply to only a part of the far field. Their focusing on a distance criterion for a given frequency to define what they call the far field

$$r >> \kappa_*^{-3}\, V_A/\Omega_i \tag{27}$$

rather obscures the decisive angle condition hidden in κ_* (expressed in (20)). For small κ_*, (18) implies (9); so that $r \cong x\frac{V_A}{V}$, thus reducing condition (27) to our (19). However, for the region well behind the wings, where $r \sim x$, (27) becomes

$$\kappa_*^3|\bar{x}| >> V_A/V, \tag{28}$$

which is more stringent than necessary, according to (19).

We have obtained approximate far-field solutions for two different domains. Interestingly, and serving to confirm the results, in cases of small κ_* for which (19) is still satisfied, one can apply the stationary-phase method to (12) and (13) and use asymptotic approximations for Airy functions to obtain expressions (25) and (26).

All frequencies in the range

$$\left(\frac{\omega}{\Omega_i}\right)^3 \le O\left(|\bar{x}|^{-1}\right) \tag{29}$$

make up the Alfvén wing, the structure of which is, as we have just shown, that of Airy functions.

CONCLUSIONS

We have derived integral expressions for the fields associated with the Alfvén wave packets excited by a constant-current tethed system operating in a uniform, infinite magnetoplasma with plasma parameters like those in the the F-layer of the Earth's ionosphere and with the geomagnetic field perpendicular to the direction of tether motion but making an arbitrary angle with respect to the horizontal plane. Taking these integrals as a starting point, we have then obtained approximate solutions for the fields far from the tethered system in two different domains.

In the Alfvén wings proper, we have identified the general structure of the fields to be that of Airy functions. That is, the variation in the Alfvén wave fields along the direction of motion of the system, far from the system and in the wings, is given by the Airy integrals Gi (for the electric field component parallel to the tether's velocity vector) and Ai (for the electric field component perpendicular to the velocity and geomagnetic field vectors). The asymptotic result also shows the Airy function amplitudes to fall off as the inverse cube root of x, the co-ordinate of the point (relative to the tether) along the axis parallel to the velocity of the system .

For the far field well behind the wings we have confirmed a previous result that in the plane of the wings, along a given ray from the contactor, the amplitude falls off as the inverse square root of the distance from the contactor, and we have obtained analytical expressions for how the field varies. We have also clarified a statement in reference 6 about the boundary of the far field.

These results could be of some practical utility in the near future, from the scientific standpoint, should efforts to obtain ionospheric plasma wave measurements by satellites during the TSS-1R mission prove successful. They also represent a step toward obtaining the Alfvén fields at the boundary with the atmosphere, a prerequisite for calculations of the field on the Earth's surface. The wave reflected at the boundary must also be taken into account for this task. Efforts are underway to make these calculations.

Because of the exponential decay of the fields as one moves away perpendicularly from the plane of a wing, for long tethers one need consider the contribution of only one wing (contactor) or the other for any point in a horizontal plane, unless the dip angle of the magnetic field is large. For TSS-1R the contribution of the wings in a given horizontal plane is always disjoint. This was not the case for the 500-meter- long tether of PMG. Our results provide the means to determine when both contributions need to be calculated in any case.

The assumption of a uniform ionosphere is among the least realistic features of our model. Future work will take into account vertical variations in plasma density, collision frequencies, etc. Since the outlook for detection on the ground of the constant-current waves is not good due to the total reflection of such waves at the atmospheric boundary[11], the TSS-1R current will be pulsed at times. Future work will consider this case and the fast magnetosonic waves, which are evanescent for constant current.

ACKNOWLEDGEMENTS

The work of R. Estes was supported in part by NASA contract NAS8-36809.

REFERENCES

1. Radiation of plasma waves by a conducting body moving through a magnetized plasma; A. Barnett and S. Olbert, *J. Geophys. Res., 91*, 10, 117 (1986)

2. Currents between tethered electrodes in a magnetized laboratory plasma; R. L. Stenzel and J. M. Urrutia, *J. Geophys. Res., 95*, 6, 209 (1990)

3. The radiation impedance of orbiting conductors; J. R. Sanmartín and M. Martinez-Sanchez, *J. Geophys. Res., 100*, 1677 (1995)

4. Drag and propulsion of large satellites in the ionosphere: An Alfvén engine in space; S. P. Drell, H. M. Foley, and M. A. Ruderman, *J. Geophys. Res., 70*, 3131 (1965)

5. Alfvén waves from an electrodynamic tethered satellite system; R. D. Estes, *J. Geophys. Res., 93*, A2, 945 (1988)

6. The excitation of plasma waves by a current source moving in a magnetized plasma: Two-dimensional propagation; C. E. Rasmussen, P. M. Banks, and K. J. Harker, *J. Geophys. Res., 95*, 10,459 (1990)

7. Estimating radiated power from a conducting tethered satellite system; D. J. Donahue,T. Neubert, and P. M. Banks, *J. Geophys. Res., 96*, 21,245 (1991)

8. Generation of plasma waves by a tethered satellite elongated in the direction of flight for arbitrary oblique geometry; A. Lüttgen and F. M. Neubauer, *J. Geophys. Res., 99*, A12, 23,349 (1994)

9. *Handbook of Mathematical Functions*, M. Abramowitz and I. Stegun, pp.446-448,Dover Publications, Inc.,New York

10. Far-wake structure in rarefied plasma flows past charged bodies; J. R. Sanmartín and S. H. Lam, *Phys. Fluids 14*, 62 (1971)

11. Calculating the electromagnetic field on the Earth due to an electrodynamic tethered system in the ionosphere; R. D. Estes, *Proceedings of the Third International Conference on Tethers in Space*, American Institute of Aeronautics and Astronautics, Inc. (1989)